Title

Clustered, Regularly Interspaced Short Palindromic Repeats (CRISPR)/Cas9-coupled Affinity Purification/Mass Spectrometry Analysis Revealed a Novel Role of Neurofibromin in mTOR Signaling*

Journal

Molecular & Cellular Proteomics, 16(4)

ISSN

1535-9476

Authors

Li, Xu
Gao, Min
Choi, Jong Min
et al.

Publication Date

2017-04-01

DOI

10.1074/mcp.m116.064543

Peer reviewed

Clustered, Regularly Interspaced Short Palindromic Repeats (CRISPR)/Cas9-coupled Affinity Purification/Mass Spectrometry Analysis Revealed a Novel Role of Neurofibromin in mTOR Signaling*[S]

Xu Li‡§¶, Min Gao‡§, Jong Min Choi‖, Beom-Jun Kim‖, Mao-Tian Zhou‡, Zhen Chen‡, Antrix N. Jain‖, Sung Yun Jung‖, Jingsong Yuan, Wenqi Wang‡‡§§¶¶, Yi Wang‖¶¶, and Junjie Chen‡¶¶**

Neurofibromin (NF1) is a well known tumor suppressor that is commonly mutated in cancer patients. It physically interacts with RAS and negatively regulates RAS GTPase activity. Despite the importance of NF1 in cancer, a high quality endogenous NF1 interactome has yet to be established. In this study, we combined clustered, regularly interspaced short palindromic repeats (CRISPR)/Cas9-mediated gene knock-out technology with affinity purification using antibodies against endogenous proteins, followed by mass spectrometry analysis, to sensitively and accurately detect NF1 protein-protein interactions in unaltered *in vivo* settings. Using this system, we analyzed endogenous NF1-associated protein complexes and identified 49 high-confidence candidate interaction proteins, including RAS and other functionally relevant proteins. Through functional validation, we found that NF1 negatively regulates mechanistic target of rapamycin signaling (mTOR) in a LAMTOR1-dependent manner. In addition, the cell growth and survival of NF1-deficient cells have become dependent on hyperactivation of the mTOR pathway, and the tumorigenic properties of these cells have become dependent on LAMTOR1. Taken together, our findings may provide novel insights into therapeutic approaches targeting NF1-deficient tumors. ***Molecular & Cellular Proteomics 16: 10.1074/mcp.M116.064543, 594–607, 2017.***

Neurofibromatosis type 1 is an autosomal dominant condition that is characterized by the development of multiple neurofibromas, Lisch nodules, scoliosis, learning disabilities, vision disorders, mental disabilities, multiple café au lait spots, and epilepsy. The average life expectancy of patients with neurofibromatosis type 1 is significantly reduced, and malignancy is the most common cause of death (1). These malignancies are caused by mutations of the *NF1* gene, which is located at chromosome 17q11.2 and encodes neurofibromin (NF1),[1] a GTPase-activating enzyme for RAS proteins (2). *NF1* is a well known tumor suppressor that is frequently mutated in many types of human cancer, such as malignant peripheral nerve sheath tumor (3), glioblastoma (4), melanoma (5), ovarian carcinoma (6), lung cancer (7), and breast cancer (8). NF1 protein physically interacts with RAS and accelerates RAS GTPase hydrolysis (9), whereas NF1-deficient cells show increased levels of RAS-GTP, which results in hyperactivation of RAS signaling (10). However, despite the importance and high alteration/mutation rate of NF1 in cancer, NF1-based therapeutic approaches are lagging behind. This is mainly due to the limited understanding of NF1 regulation and its additional functions other than regulating KRAS. Several clinical trials targeting the Ras pathway in patients carrying *NF1* mutations showed at best minor responses (11). Combined

From the ‡Department of Experimental Radiation Oncology, University of Texas M.D. Anderson Cancer Center, Houston, Texas 77030; ‖Department of Molecular and Cellular Biology, Baylor College of Medicine, Houston, Texas 77030; **Department of Radiation Oncology, Center for Radiological Research, Columbia University, New York, New York 10032; ‡‡Department of Developmental and Cell Biology, University of California at Irvine, Irvine, California 92697

Received October 6, 2016, and in revised form, January 25, 2017
Published, MCP Papers in Press, February 7, 2017, DOI 10.1074/mcp.M116.064543
Author contributions: X. L., S. J., J. Y., W. W., Y. W., and J. Chen designed the research; X. L., M. G., B. K., M. Z., Z. C., and W. W. performed research; X. L., J. Choi, M. Z., A. N. J., and S. Y. J. analyzed data; X. L. and J. Chen wrote the paper.

[1] The abbreviations used are: NF1, neurofibromin; AP-MS, affinity purification followed by mass spectrometry; AP, affinity purification; HCIP, high-confidence candidate interacting protein; LAMTOR1, late endosomal/lysosomal adaptor, MAPK and mTOR activator 1; mTOR, mechanistic target of rapamycin; PPI, protein-protein interaction; PSM, peptide spectrum match; SFB, S tag-FLAG tag-SBP tag; SILAC, stable isotope labeling with amino acids in cell culture; gRNA, guide RNA; S6K, S6 kinase; IP, immunoprecipitation; AMPK, AMP kinase.

therapies targeting more than one node in the cell proliferation pathway have been proposed, because inhibiting a single node may lead to activation of compensatory negative feedback pathways. However, to effectively target NF1-related cancers, a better understanding of NF1 functions and regulations is needed.

Because protein-protein interactions imply functional connections between proteins, learning what NF1 interacts with and how these interactions contribute to NF1 functions may greatly increase our understanding of this protein. However, NF1-interacting proteins remain largely unknown, because NF1 is a very large protein, with 2818 amino acids and an estimated molecular mass of 327 kDa. It is technically challenging to express NF1 full-length protein exogenously in mammalian cells. Moreover, although the NF1-RAS axis has long been known as one of the most important regulators of RAS signaling in many types of cancer, all previous NF1 interaction studies have failed to detect the NF1-RAS interaction (12), probably because of the transient nature of this enzyme-substrate interaction. A high quality NF1 endogenous interactome will reveal additional details about NF1's functions and regulations and should greatly increase our understanding of its biology and involvement in diseases.

As an unbiased approach, affinity purification followed by mass spectrometry (AP-MS) offers tremendous advantages over other methods in identifying protein-protein interactions (PPIs) under near-physiological conditions and identifying protein complexes instead of binary interactions (13). By performing AP of a protein of interest (the "bait"), followed by LC-MS/MS, the partner proteins (the "prey") that form complexes with the bait can be identified (14). AP-MS has been employed to study individual proteins in different signaling events, such as the TGF-β and Wnt signaling pathways (15–21). We have used this approach to study the DNA damage-signaling pathways. Many insights into the regulation of DNA damage-responsive pathways have been initiated on the basis of the AP-MS results of individual DNA damage-responsive proteins (22–26). In mammalian cells, overexpression of tagged proteins is most commonly used. However, several limitations compromise AP-MS quality, including high false-positive rates and overexpression artifacts that disrupt protein balance and complex assembly (27). Moreover, overexpression of bait protein often saturates the system and impedes capture of the dynamic changes in PPIs in response to certain biological stimuli (28).

Ideally, AP-MS using antibodies that recognize endogenous proteins are the better choice than the overexpression system, because they cause minimal disturbance to the system and may avoid overexpression artifacts. However, the major drawback of using antibodies against endogenous proteins in AP-MS is that they often pull down a significant number of nonspecific cross-reactive binding proteins, which are impossible to eliminate through a bioinformatics analysis and are detrimental to the quality of MS results (13).

To effectively eliminate contaminants while preserving weak interactions and avoiding extensive control experiments, a series of methods based on isotope-labeled quantitative MS has been proposed (29–33). All of them use stable isotope labeling with amino acids in cell culture (SILAC) for the quantitative measurement of the relative amount of proteins. For instance, Selbach and Mann (32) developed a method named "QUICK" (quantitative immunoprecipitation combined with kknockdown) that couples RNA interference and SILAC. The authors used extracts prepared from cells with 90% down-regulation of β-catenin expression and found that the antibodies against the endogenous protein (*i.e.* β-catenin) pulled down less β-catenin and four of its associated proteins than did wild-type cells. The differences in binding proteins were quantitatively captured by SILAC. We believe that the incomplete removal of the bait proteins by small interfering RNA or short hairpin RNA has limited the application of this method. Because AP can greatly enrich the bait protein, even a small amount of leftover bait protein could be enriched to a level comparable with that in wild-type cells. Thus, this method still brings down a significant number of *bona fide* interacting proteins in control AP-MS and therefore may generate considerable false-negatives. A cleaner background is a must if we would like to more sensitively and accurately detect interactions.

First demonstrated as a genome engineering/editing tool in human cell cultures in 2012 (34), clustered regularly interspaced short palindromic repeat (CRISPR)/Cas9 technology has become a rapid and precise method of editing DNA in human cells and in animals (35, 36). The Cas9 nuclease targets the protospacer adjacent motif sequence introduced by the predesigned guide RNA (gRNA) and cuts 3–4 nucleotides upstream of the protospacer adjacent motif sequence, which sometimes leads to frameshift mutations and subsequent silencing of target genes. Here, we combined CRISPR/Cas9 gene knock-out technology with modified AP-MS protocols, and we used antibodies against endogenous proteins to sensitively and accurately detect NF1 protein-protein interactions under endogenous settings.

EXPERIMENTAL PROCEDURES

Cell Culture, Constructs, Transfection, and Virus Packaging—HeLa and HEK293T cells were cultured in Dulbecco's modified Eagle's medium, supplemented with 10% fetal bovine serum and 1% penicillin and streptomycin. MCF10A cells were cultured in Dulbecco's modified Eagle's medium/F-12, supplemented with 5% horse serum, 10 μg/ml insulin, 20 μg/ml epidermal growth factor, 0.5 μg/ml hydrocortisone, 0.1 μg/ml cholera toxin, and 1% penicillin and streptomycin.

The plasmids encoding the indicated SFB-tagged genes were obtained from the Human ORFeome V5.1 library or purchased from Open Biosystems and recombined into a gateway-compatible destination vector to determine the expression of C-terminal SFB-tagged fusion proteins. The human codon-optimized Cas9 construct and the target gRNA expression construct were obtained from Addgene and deposited by Dr. George M. Church (36). The NF1 gRNA sequences

were introduced into the expression construct by site-directed mutagenesis polymerase chain reaction. The gRNA sequences against NF1 are 5′-AAGCTATTTGACTTGGTGGA-3′ and 5′-GTTAGCAGTTATAAATAGCC-3′.

Constructs encoding Cas9 and gRNA were co-transfected with pCDNA3-EGFP into HEK293T cells using polyethyleneimines, as described previously (37). Cells were sorted on the basis of their GFP signal, and single clones were chosen. The knock-out clones were confirmed by Western blotting and sequencing.

All lentiviral supernatants were generated by transient transfection of HEK293T cells with the helper plasmids pSPAX2 and pMD2G (kindly provided by Dr. Zhou Songyang) and harvested 48 h later. Supernatants were passed through a 0.45-μm filter and used to infect HEK293T and HeLa cells, with the addition of 8 μg/ml Polybrene.

Western Blotting, Pulldown, and Immunoprecipitation Assays—Whole cell lysates were prepared by lysing cells with NETN buffer (20 mM Tris-HCl (pH 8.0), 100 mM NaCl, 1 mM EDTA, and 0.5% Nonidet P-40) on ice for 30 min and then boiling them in 2× Laemmli buffer. Lysates were subjected to SDS-PAGE, followed by immunoblotting with antibodies against various proteins, including NF1 (Abcam, ab17963) and KRAS (Abcam, ab55391); β-tubulin (Sigma-Aldrich, T8328) and FLAG M2 (Sigma-Aldrich, F3165); LAMTOR1 (Cell Signaling 8975), mTOR, Raptor, Rictor, and GβL (Cell Signaling, 9964), TSC1 (Cell Signaling 6935), TSC2 (Cell Signaling 3612), AMPKα1/2 and AMPKβ1/2 (Cell Signaling 9957), and phospho-p70 S6 kinase (Thr-389) (Cell Signaling 9205).

For the pulldown, immunoprecipitation, and co-immunoprecipitation (co-IP) assays, 1×10^7 cells were lysed with NETN buffer on ice for 30 min. The lysates were then incubated with 20 μl of conjugated S-beads (for SFB-tagged pulldown) for 2 h at 4 °C or incubated with antibodies against endogenous proteins for 1 h at 4 °C, followed by the addition of 20 μl of protein A/G-agarose, and incubated for 2 h at 4 °C. Beads were washed three times with NETN buffer and boiled in 2× Laemmli buffer.

AP of Endogenous NF1 Protein Complexes, MS Analysis, and Data Analysis—A streamlined workflow of CRISPR/Cas9-coupled AP-MS can be found in the supplemental material.

We lysed 1×10^8 HeLa, HEK293T, or MCF10A cells with NETN buffer (20 mM Tris-HCl (pH 8.0), 100 mM NaCl, 1 mM EDTA, and 0.5% Nonidet P-40, containing 1 μg/ml each of pepstatin A and aprotinin) for 30 min. Crude lysates were centrifuged at 16,000 × *g* for 15 min. The supernatants were transferred to a new tube and incubated with NF1 (Ab1, Abcam, ab17963; Ab2, Bethyl, A300-140A) or KRAS (Abcam, ab55391) antibodies for 1 h at 4 °C, followed by centrifugation at 100,000 × *g* for 15 min. The supernatant was again transferred to a new tube and incubated with 30 μl of protein A beads for 1 h at 4 °C. The supernatant was discarded, and the beads were washed three times with 1 ml of ice-cold NETN buffer, boiled in 40 μl of 2× Laemmli buffer, and subjected to SDS-PAGE. The protein band containing the entire sample was excised and cut into four pieces from top to bottom. The gel pieces were then subjected to in-gel trypsin digestion and vacuum dried. Samples were reconstituted in 6 μl of high performance liquid chromatography (HPLC) solvent A (2.5% acetonitrile and 0.1% formic acid), and the top two bands and bottom two bands were combined into two samples. A nano-scale reverse-phase HPLC capillary column was created by packing 5-μm C18 spherical silica beads into a fused silica capillary (100-μm inner diameter × ~20-cm length) with a flame-drawn tip. After the columns had been equilibrated, each sample was loaded onto the column. A gradient was formed, and peptides were eluted with increasing concentrations of solvent B (97.5% acetonitrile and 0.1% formic acid). As the peptides eluted, they were subjected to electrospray ionization and then entered into an LTQ-Orbitrap Velos mass spectrometer (Thermo Fisher Scientific, San Jose, CA) with a 75-min acetonitrile gradient. The peptides were detected, isolated, and fragmented to produce a tandem mass spectrum of specific fragment ions. The raw data were collected in a data-dependent mode in which the precursors were scanned by the Orbitrap (target resolution 100 K), fragmented by collision-induced dissociation, and analyzed by LTQ-Velos. The survey scan was limited to 375–1300 *m/z*. Peptide sequences (and hence protein identity) were determined by matching the acquired fragmentation pattern with human reference protein databases using the Mascot 2.4 program (Matrix Science) in Proteome Discoverer 1.4 software (Thermo Fisher Scientific). Enzyme specificity was set to semi-tryptic, with two missed cleavages. Modifications included oxidation (methionine, variable) and ^{13}C-K (SILAC, variable). Mass tolerance was set to 20 ppm for precursor ions and 0.5 Da for fragment ions. A search was performed using the in-house human reference database (total 73,637 entries) based on the database downloaded from NCBI (2015-0610). Spectral matches were filtered to contain less than 1% FDR at the peptide level on the basis of the target-decoy method. The protein inference was evaluated following the general rules reviewed in Ref. 38, with manual annotation based on experience when necessary. When peptides matched multiple proteins, they were assigned to only the most logical protein (parsimony principle). However, all possible proteins were considered when the results from WT and KO cells were compared. To generate HCIPs, all the data were applied to a 1% protein FDR filter, and peptide spectral matches were used. This same principle was used for isoforms, when present in the database. For label-free quantitation of MS1 peak areas, we used the outputs from quantitative Proteome Discoverer 1.4. To get the reproducible protein IDs, we used Perl-based, in-house label-free quantification software, which matches the peaks from the two replicates/injections. The reported protein IDs were identified in Mascot/PD with at least two peptide spectrum matchs (PSMs) in at least one replicate/injection; and the corresponding peaks can be matched in the other sample with the same *m/z* and similar retention time. For SILAC data quantitation, the searched peptide information was imported into Skyline software, followed by importing the raw data. Peptide MS1 peak area quantitation was performed as described previously (39, 40). Manual adjustments of peak selections were performed when necessary.

We downloaded protein sequences and annotations from the UniProt Consortium (41). The heat maps were generated using Multi Experiment Viewer version 4.9.0 software. The pathway annotations and disease correlations were generated using the HCIPs identified in our studies, weighted by the spectra counts. We then estimated the significance of these correlations using the Knowledge Base provided by Ingenuity pathway software (Ingenuity Systems), which contains findings and annotations from multiple sources, including the Gene Ontology database. We used the $-\log(p \text{ value})$ of individual functions to create disease annotation networks. The HCIP disease network was visualized using Cytoscape software (42).

Experimental Design and Statistical Rationale—All MS experiments were repeated twice (biological repeats). Each experiment contained two MS injections, and the raw files were combined and searched together. There were 16 label-free NF1 AP-MS, 4 NF1 SILAC-AP-MS, and 2 reciprocal KRAS AP-MS experiments. The knock-out cells were used as negative controls of MS. All other experiments were repeated three times. No samples were excluded from the analysis. Differences between groups were analyzed using Student's *t* test and Pearson χ^2 analysis. A p value < 0.05 was considered statistically significant unless otherwise specified. When calculating the p values for gene ontology annotations, a Fisher's exact test was used.

Soft Agar Colony Formation Assay—HeLa cells (1×10^3) were added to 1.5 ml of growth medium with 0.2% agar and layered onto 2 ml of a 0.5% agar bed in 6-well plates. The medium was replenished every 3 days for 14 days. The resulting colonies were fixed and

stained with Crystal Violet. The numbers of colonies were counted with a GelDoc using Quantity One software (Bio-Rad).

RESULTS

Investigate NF1 Endogenous Protein Complexes in HeLa Cells—To establish a high quality endogenous NF1 interactome, we used a CRISPR/Cas9 gene editing system to generate knock-out cells as negative controls, followed by AP-MS using a modified protocol. In brief, knock-out cells were generated using the CRISPR/Cas9 system, as described previously (35). Endogenous protein complexes were affinity purified from extracts prepared from wild-type and knock-out cells using the same antibodies against endogenous protein and analyzed via MS, following the workflow for the identification of protein complexes that we previously established (43, 44). Prey proteins identified from MS results were classified into three groups as follows: orange, *bona fide* interacting proteins; green, proteins that bind to the antibodies but not to the bait (cross-reactive binding proteins); and purple, generic preys (for example, heat-shock proteins and other nonspecific binding proteins (actin, tubulin, and ribosomal proteins)) that are frequently detected via AP-MS (Fig. 1*A*). The *bona fide* interacting proteins should only exist in the immunoprecipitates of extracts prepared from wild-type cells, whereas the other two groups of proteins exist comparably in the immunoprecipitates of both wild-type and knock-out cell extracts. By comparing the results from wild-type cells and knock-out control cells, we could easily distinguish *bona fide* interacting proteins from strong background noise (Fig. 1*A*). We termed this new method "affinity purification/mass spectrometry in CRISPR/Cas9 utilizing systems for mapping endogenous protein complexes (ACUMEN)." The detailed step-by-step protocol can be found in the supplemental material.

NF1 is ubiquitously expressed in almost all human tissues and performs tumor suppressor functions, mutations of which were found in many types of cancers (11, 12). One of the early studies of NF1-KRAS interaction was performed in HeLa cells (10). They identified and confirmed NF1-KRAS interaction by immunoprecipitation-Western analysis using antibodies against NF1 protein in HeLa cells. Our whole proteome profiling data of HeLa cells confirmed it expressed adequate amounts of NF1 and KRAS proteins, which are detectable by MS. Thus, we started by establishing the endogenous NF1 interactome using HeLa cells.

Using CRISPR/Cas9 technology, we generated NF1-knock-out HeLa cells. We first designed gRNAs that target different exons of the *NF1* gene, engineered them into a gRNA expression vector through site-directed mutagenesis (36), and co-transfected them with a vector coding human codon-optimized Cas9 and enhanced green fluorescent protein into HeLa cells. After sorting for green fluorescent protein, we seeded cells into 96-well plates and screened colonies via Western blotting (Fig. 1*B*). Knock-out clones (numbers 8 and 12) were further validated by sequencing to confirm frameshift

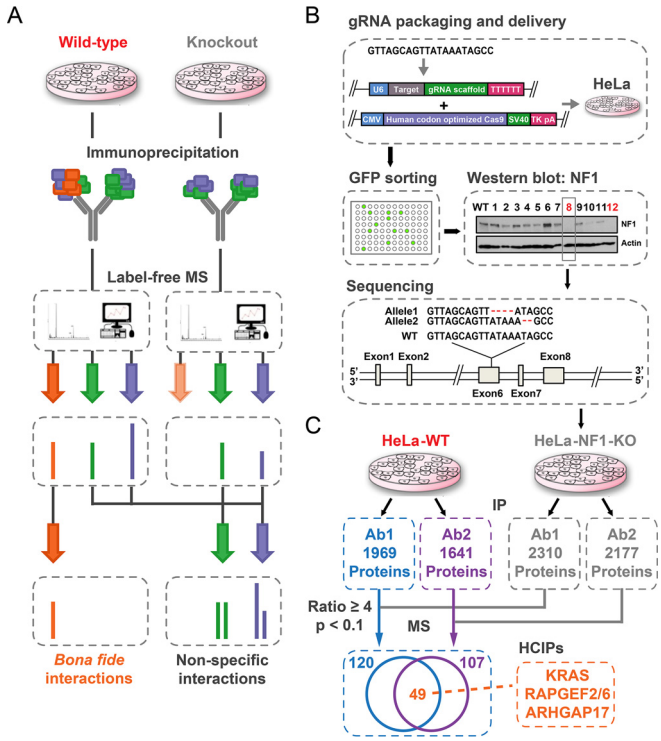

FIG. 1. **Integrated view of the use of ACUMEN to investigate endogenous protein complexes.** *A,* label-free CRISPR/Cas9-coupled AP-MS. Step 1, generate knock-out cells using the CRISPR/Cas9 system. Step 2, AP-MS of wild-type and knock-out cells. Step 3, data analysis. Prey proteins identified from MS results can be classified into three groups: *orange*, *bona fide* interacting proteins; *green*, cross-reactive binding proteins; and *purple*, generic preys and other nonspecific binding proteins. *B* and *C,* schematic shows the major steps involved in CRISPR/Cas9-coupled AP-MS and data analysis of NF1 and a snapshot of each part of the data.

mutations. We observed that both alleles were frameshift-mutated in clone no. 8, and we used this clone as the NF1-knock-out HeLa cells for all following experiments (Fig. 1*B*). We then performed AP using two different antibodies (Ab1, Abcam, ab17963; Ab2, Bethyl, A300-140A) against the same region of endogenous NF1 (residue 2760–2818), side by side in wild-type (HeLa-WT) and NF1-knock-out (HeLa-NF1-KO) HeLa cells (Fig. 1*C*), using a modified AP protocol that was designed to capture the binding proteins at the maximum capacity without attempting to limit the background contamination (supplemental material). We hoped this process could preserve the weak and transient interactions at the maximum capacity of MS instruments and thus take full advantage of the instruments.

The immunoprecipitated complexes were subjected to MS using a label-free shotgun method on a Linear Trap Quadrupole-Orbitrap Velos mass spectrometer (Thermo Fisher Scientific), searched with Mascot (45), and quantitated with PSMs and peak areas (supplemental Table 1). This new method generated about 2000 interacting proteins from every AP-MS experiment, which is reproducible in both replicates

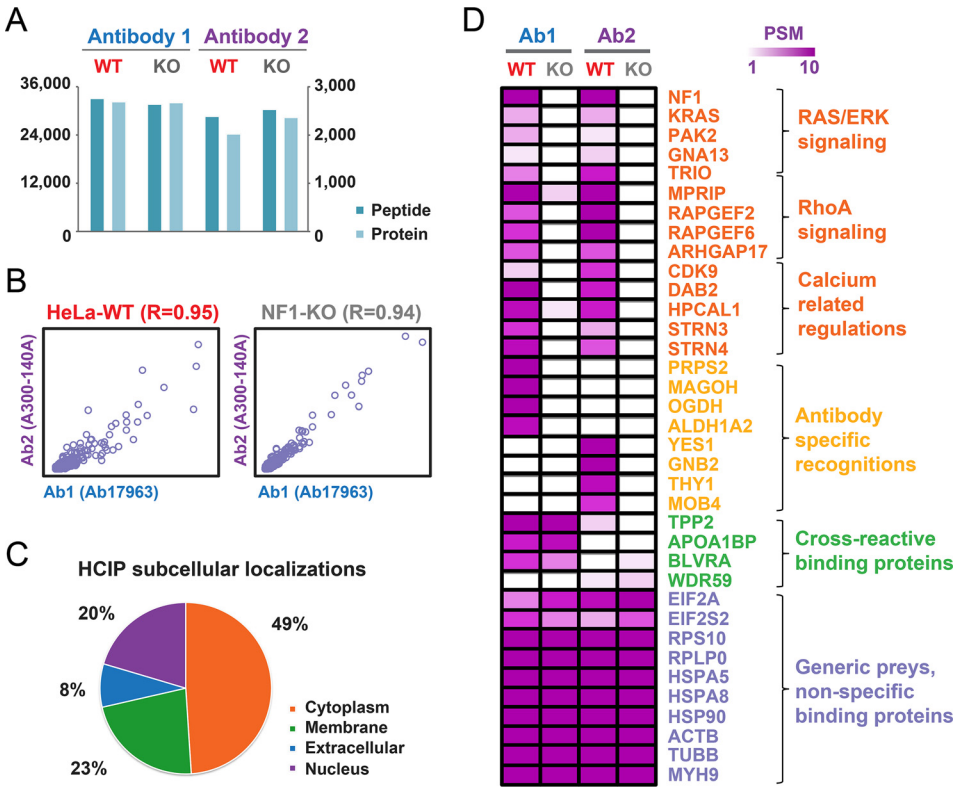

FIG. 2. **Summary of NF1 AP-MS results in HeLa cells.** *A,* total protein and peptide identifications in each experiment are summarized. *B,* correlation between AP-MS results using two NF1 antibodies. *x* and *y* axes indicate the PSMs of proteins identified in the indicated experiments. *C,* major subcellular localizations of HCIPs are summarized. *D,* heat map of the relative abundance of the indicated proteins representing the four groups that were categorized on the basis of their specificities: HCIPs (*orange*); specific interacting proteins detected by one antibody (*yellow*); cross-reactive binding proteins (*green*); and generic preys and other nonspecific binding proteins (*purple*) in different experiments. Proteins were also categorized into functional groups.

and at least recovered 2 PSM in one replicate (Fig. 1*C*), which was at least twice that of a previous one-step or tandem AP-MS strategies (37, 43, 46–49). Both antibodies recovered a reasonable amount of NF1 from HeLa-WT cells (Ab1, 161 PSM; Ab2, 287 PSM) but almost no NF1 from HeLa-NF1-KO cells (Ab1, 1 PSM; Ab2, 0 PSM), indicating that the NF1 protein complex is completely missing in the protein complexes pulled down in HeLa-NF1-KO cells (Fig. 1*C* and supplemental Table 1).

Only 120 and 107 proteins, respectively, were enriched in WT cells by NF1 antibodies Ab1 and Ab2, using a cutoff of four normalized protein fold changes and $p < 0.1$, with peak alignment across all experiments (Fig. 1*C*). The lists of proteins that had been identified using two different antibodies showed a high degree of overlap; 86% of proteins were also enriched by other antibodies, although many did not reach our stringent cutoff threshold. This finding indicates that the cross-reactions by particular antibodies can be successfully eliminated using this approach (Fig. 1*C* and supplemental Table 2). Forty nine proteins that showed up in both lists were considered to be the most confident NF1 HCIPs, including KRAS, the GTPase-regulating guanine nucleotide exchange factors RAPGEF2 and RAPGEF6; Trio, the Rho GTPase-activating protein ARHGAP17; and other GTPase-interacting proteins, such as GNA13, MPRIP, ERC1, and PAK2 (supplemental Table 2). All of which are likely *bona fide* NF1-binding partners because of their ability to regulate GTPases. None of these proteins have been identified in any previous NF1 AP-MS studies (12).

Both antibodies recovered similar amounts of total proteins and PSMs (Fig. 2*A*), indicating that the majority of NF1-interacting proteins identified by AP-MS were nonspecific. The NF1-associated proteins detected by two different antibodies showed a high degree of similarity. The overall correlation *R* values in HeLa-WT and HeLa-NF1-KO cells were estimated to be 0.95 and 0.94, respectively, suggesting excellent data reproducibility in this study (Fig. 2*B*). As predicted, most HCIPs were localized in the cytoplasm (49%) and plasma membrane (23%) (Fig. 2*C*). Proteins were also categorized into groups on the basis of their presence in WT and KO cells as follows: *bona fide* HCIPs (*orange*), specific interacting proteins detected by one antibody (*yellow*), cross-reactive binding proteins (*green*), and generic preys and other nonspecific binding proteins (*purple*) (Fig. 2*D*). A large number of the novel NF1 HCIPs that were specifically recognized using ACUMEN methods are involved in RAS/ERK signaling, RhoA signaling,

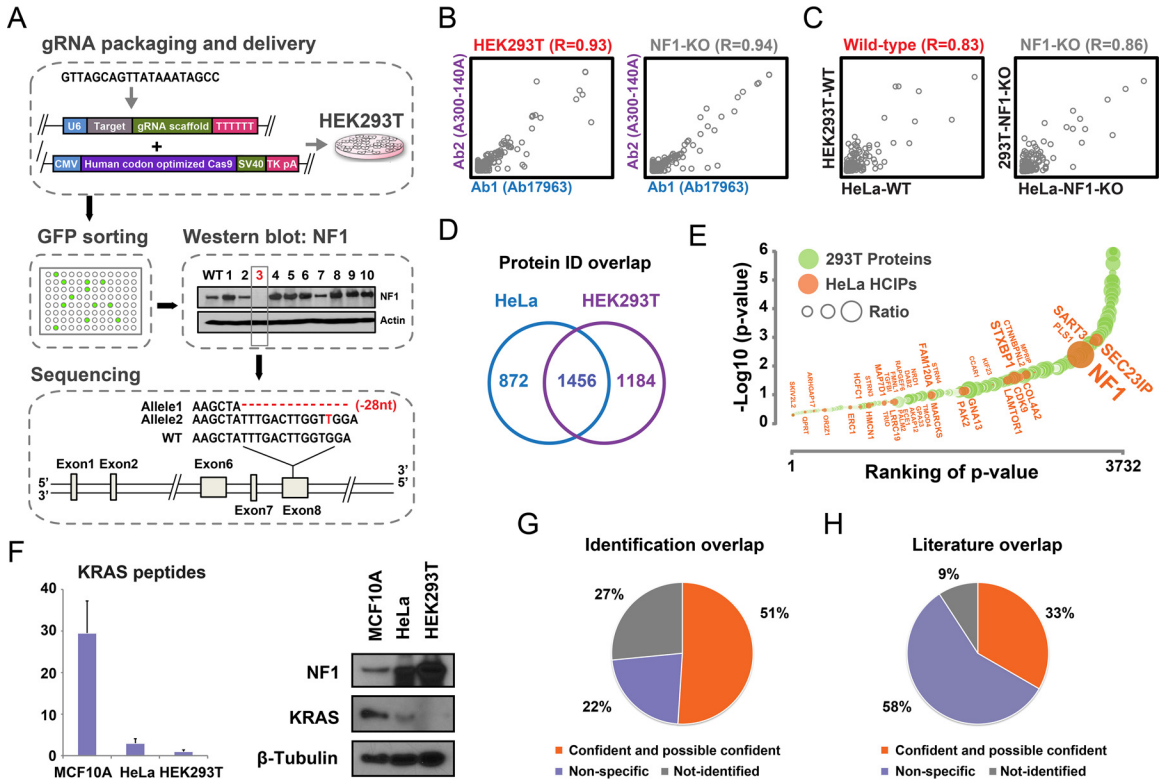

FIG. 3. **Summary of NF1 AP-MS results in HEK293T cells and data comparisons between the two cell lines and literatures.** *A,* schematic shows the major steps involved in establishing HEK293T-NF1-KO cells using the CRISPR/Cas9 system and a snapshot of each part of the data. *B,* correlation between AP-MS results using two NF1 antibodies in HEK293T and HEK293T-NF1-KO cells. *x* and *y* axes indicate the PSMs of proteins identified in the indicated experiments. *C,* correlation between AP-MS results from HEK293T and HeLa cells and results from HEK293T-NF1-KO and HeLa-NF1-KO cells. *x* and *y* axes indicate the PSMs of proteins identified in the indicated experiments. *D,* Venn diagrams summarizing the results obtained from 293T and HeLa cells. *E,* prey specificity map of NF1-interacting proteins identified in HEK293T cells. The size of the dots indicates the ratio of protein abundance between WT and NF1-KO cells. Proteins that also exist in HeLa HCIPs are labeled as *orange*. *F, left panel,* KRAS expression in different cell lines was evaluated by bait peptide recoveries from KRAS purification. The *y* axis indicates the average spectra counts of KRAS protein. *Right panel,* NF1 and KRAS protein levels were also evaluated by Western blotting in MCF10A, HeLa, and HEK293T cells, using β-tubulin as the internal control. *G,* overlap between NF1 HCIPs in HeLa cells and the results from HEK293T cells. The HeLa HCIPs with 2-fold enrichment of HEK293T cells compared with HEK293T-NF1-KO cells and $p < 0.1$ were considered as possible confident. *H,* literature overlap data in supplemental Table S6 are summarized.

and calcium-related regulations, which are all NF1 known functions (Fig. 2*D*). Our findings suggest that novel molecular mechanisms underlie these regulations. Because proteins encoded by mutated genes in inherited genetic disorders are likely to interact with proteins known to cause similar disorders, suggesting the existence of disease PPI subnetworks (50), we further analyzed the correlations between diseases and NF1 HCIPs (supplemental Table 3) and built an NF1 HCIP-cancer network (supplemental Fig. S1). Indeed, many HCIPs are involved in glioblastoma, astrocytoma, and blood cancers, which are known to have NF1 mutations (51). Our findings also suggest links between NF1 and liver and reproductive system cancers, which may lead to the discovery of novel functions of NF1 in these types of cancers (supplemental Fig. S1).

Investigate NF1 Endogenous Protein Complexes in HEK293T Cells and Compare the NF1 Interactomes in the Two Cell Lines—To establish NF1 endogenous protein complexes and to evaluate ACUMEN performance in different cell lines, we performed CRISPR/AP-MS in HEK293T cells, which express similar levels of NF1 but lower levels of KRAS, following the same workflow (Fig. 3*A*). GFP-positive clone no. 3 was further validated by sequencing to confirm frameshift mutations in both alleles of *NF1* gene. Therefore, we used this clone as the NF1-knock-out HEK293T cells for all subsequent experiments (Fig. 3*A*). Following the same ACUMEN workflow, we identified similar amounts of NF1-interacting proteins using both antibodies (supplemental Table 4). The overall correlation *R* values in HEK293T-WT and HEK293T-NF1-KO cells were estimated to be 0.93 and 0.94, respectively, again indicating high data reproducibility between experiments (Fig. 3*B*). The overall correlation *R* values in two wild-type cells and two knock-out cells were estimated to be 0.83 and 0.86, respectively (Fig. 3*C*). 58% of the total protein IDs were recovered in both cell lines (Fig. 3*D*). Although NF1-RAS interaction was not detected in HEK293T cells, probably because of the lower

expression of KRAS in these cells, many other interactions remained (Fig. 3*E*). For example, the KRAS expression level was much lower in HEK293T cells than that in HeLa and MCF10A cells (Fig. 3*F*). We further confirmed the NF1-RAS interaction by performing reciprocal AP-MS following the same AP protocol, using KRAS as bait in MCF10A cells that expressed higher levels of endogenous RAS (supplemental Table 5). Most HCIPs identified in HeLa cells remained statistically significant when identified in HEK293T cells (Fig. 3*E*). Among the HeLa HCIPs identified in HEK293T cells (73% in total), 70% (51% in total) were significantly changed between wild-type and control cells (Fig. 3*G*). Combining the results from two cell lines, we recovered most of the previously reported PPIs using NF1 as the bait (Fig. 3*H*, supplemental Table 6). More importantly, we found that more than half (58%) of the NF1 "confident" interacting proteins identified in previous studies were likely to be false positives, which existed, with similar abundance, in IP complexes isolated from both WT and NF1-KO cells (Fig. 3*H*, supplemental Table 6). Collectively, these results suggest that the ACUMEN method generates fewer false positives than do previous methods while preserving more *bona fide* interacting proteins.

Using SILAC-ACUMEN to Investigate NF1 Endogenous Protein Complexes in HeLa Cells—To further validate the NF1 interactome we obtained in HeLa cells using label-free quantitative AP-MS, we performed SILAC-ACUMEN using [^{13}C]lysine-labeled HeLa and unlabeled HeLa-NF1-KO (WT(H) + NF1-KO(L)) cells and [^{13}C]lysine-labeled HeLa-NF1-KO and unlabeled HeLa (WT(L) + NF1-KO(H)) cells (Fig. 4*A*). HeLa and HeLa-NF1-KO cells were differentially labeled by being grown in medium containing unlabeled (light) or [^{13}C]lysine-labeled (heavy) amino acids for 10 generations. Affinity purifications were performed using the same antibodies against endogenous proteins (Abcam). The immunoprecipitates were mixed at a 1:1 ratio and analyzed via MS, followed by a data analysis (Fig. 4*A* and supplemental Table 7). Labeling efficiency was evaluated by comparing the heavy and light peak areas of 20 randomly chosen lysine-containing peptides in [^{13}C]lysine-labeled HeLa and HeLa-NF1-KO cells. The labeling efficiencies were over 97% in both cell lines (Fig. 4*B*). Knock-out efficiency was evaluated by comparing the peak areas of 10 randomly picked NF1 lysine-containing peptides in unlabeled HeLa and HeLa-NF1-KO cells (light) and [^{13}C]lysine-labeled HeLa and HeLa-NF1-KO cells (heavy). The knock-out efficiencies were over 98% in both unlabeled and labeled HeLa-NF1-KO cells (Fig. 4*C*).

MS results from [^{13}C]lysine-labeled HeLa cells and unlabeled HeLa-NF1-KO cells (WT(H) + NF1-KO(L)) and [^{13}C]lysine-labeled HeLa-NF1-KO and unlabeled HeLa cells (WT(L) + NF1-KO(H)) were analyzed using Proteome Discoverer software to choose the lysine-containing peptides from the proteins of interest. The chosen peptides were imported to Skyline software, and raw data were remapped to select the peaks. Peptides of NF1, KRAS, CTTNBP2NL, and HSPA5 were quantitated and visualized (Fig. 4*D*). Although peptides from NF1, KRAS, and CTTNBP2NL were highly enriched (>40-fold) in labeled forms (heavy) in (WT(H) + NF1-KO(L)) experiments and in unlabeled forms (light) in (WT(L) + NF1-KO(H)) experiments, the HSPA5 peptides showed similar intensities in both forms in both experiments (< 2-fold) (Fig. 4*D*). These results indicate that specific binding proteins can be easily distinguished from background contaminants.

Taken together, these data confirmed that our ACUMEN method also works efficiently in labeled quantitative AP-MS. The ACUMEN method could be combined with SILAC or other labeling methods, such as isobaric tags for relative and absolute quantification (52) and tandem mass tags (53, 54) for more accurate quantitation.

NF1 Forms a Stable Complex with LAMTOR1 and Negatively Regulates the mTOR Signaling Pathway—To experimentally verify the HCIP list identified using our ACUMEN method, we performed reciprocal pulldown assays by transfecting 12 SFB-tagged HCIPs, including CDK9, TGFBI, LAMTOR1, GNA13, CTTNBP2NL, DAB2, HCFC1, PAK2, STRN3, TMOD4, GPA33, and FMNL1, into HEK293T cells and pulled down with S-beads. We used empty vector and FOXR2 as negative controls. All 12 HCIPs were able to pulldown endogenous NF1 (Fig. 5*A*), which further validated that our purification results reflect endogenous PPIs under physiological conditions.

A signaling pathway annotation of NF1 HCIPs indicated that NF1 HCIPs were enriched in the mTOR signaling pathway. mTOR has been reported to be constitutively activated in *Nf1*-deficient primary cells (55); however, the molecular mechanism that underlies it remains elusive. We determined whether NF1 regulates mTOR activation through its direct binding to key components in the mTOR signaling pathway. Indeed, we found that LAMTOR1, an important component of the mTOR signaling pathway, was an NF1 HCIP; its binding with NF1 was confirmed by co-IP assay (Fig. 5*A* and supplemental Table 2). Its peptide numbers and peak areas were both highly enriched in the protein complexes pulled down in HeLa-WT and HEK293T-WT cells, but they were almost not present in HeLa-NF1-KO and HEK293T-NF1-KO cells, indicating that it specifically binds to NF1 (Fig. 5*B*). Therefore, we reciprocally confirmed that LAMTOR1 forms a stable complex with NF1 using exogenous and endogenous LAMTOR1 (Fig. 5, *C* and *D*). We further performed co-IP assays using NF1 antibodies and blotted with antibodies targeting other major components in the mTOR signaling pathway, including mTOR, TSC1/2, Raptor, Rictor, GβL, AMPKα, and AMPKβ (Fig. 5, *E* and *F*). NF1 did not form a protein complex with any of these other key components in the mTOR pathway (Fig. 5, *E* and *F*).

LAMTOR1 localizes on the surface of late endosomes and lysosomes and provides an essential anchor for a scaffold complex for the mTORC1 and MAPK pathways, which contain LAMTOR1, LAMTOR2, LAMTOR3, LAMTOR4, and LAM-

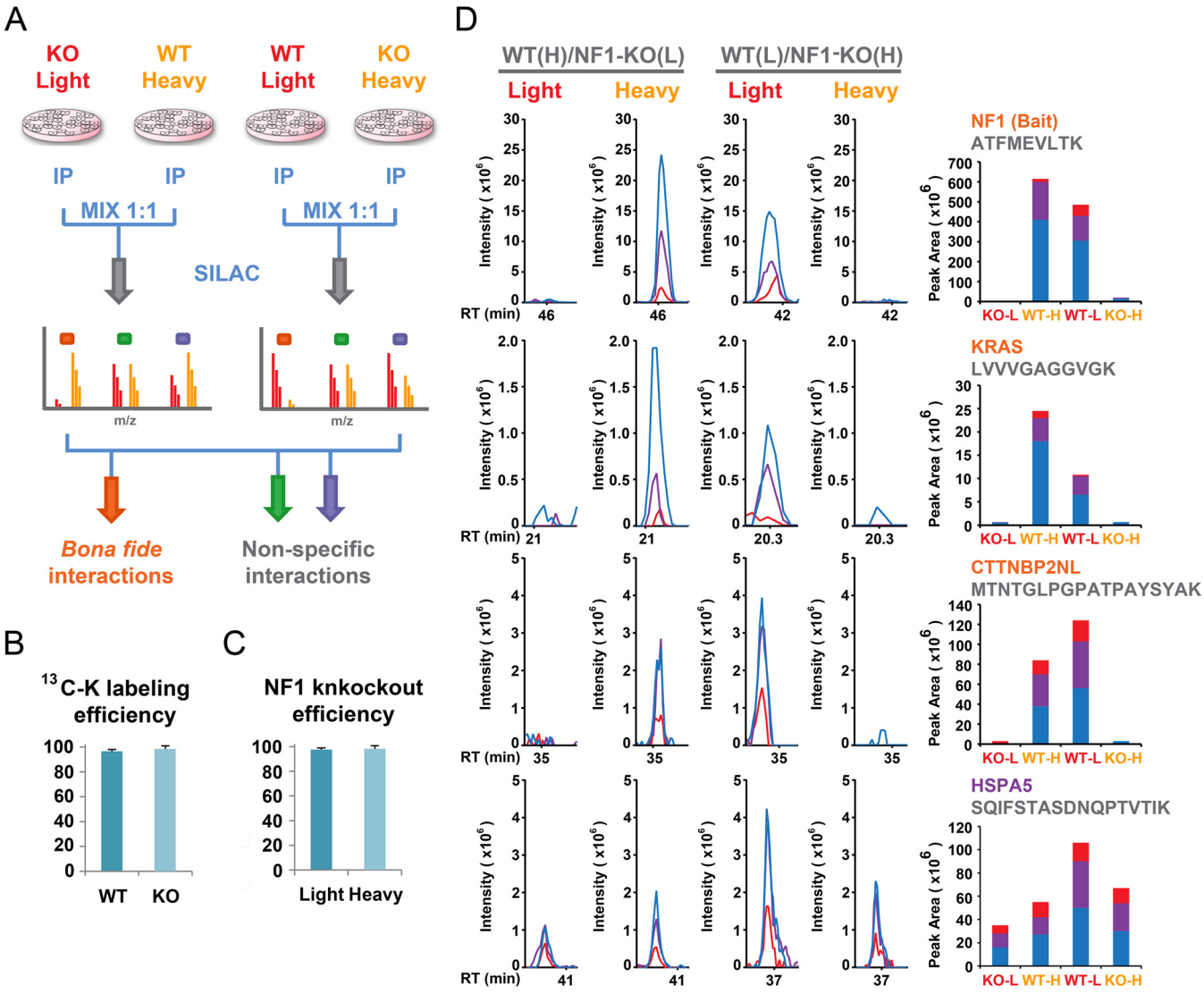

FIG. 4. **CRISPR/Cas9-coupled SILAC AP-MS studies of endogenous NF1 complexes in HeLa cells.** *A,* SILAC-labeled CRISPR/Cas9-coupled AP-MS. WT and KO cells were differentially labeled by being grown in medium containing unlabeled (light) or [^{13}C]lysine-labeled (heavy) amino acids. AP was performed using the same antibodies against endogenous proteins. The immunoprecipitates were mixed at a 1:1 ratio and analyzed via MS, followed by data analysis. *B,* labeling efficiency was evaluated by comparing the heavy and light peak areas of 20 randomly chosen lysine-containing peptides in [^{13}C]lysine-labeled HeLa and HeLa-NF1-KO cells. *C,* knock-out efficiency was evaluated by comparing the peak areas of 10 randomly chosen NF1 lysine-containing peptides in unlabeled HeLa and HeLa-NF1-KO cells (*light*) and [^{13}C]lysine-labeled HeLa and HeLa-NF1-KO cells (*heavy*). *D,* HeLa-WT and NF1-KO cells were differentially labeled. Extracts were prepared, affinity purified with NF1 antibodies, mixed at a 1:1 ratio, and analyzed by MS. Peptides of NF1, KRAS, CTTNBP2NL, and HSPA5 were quantitated and visualized using Skyline software.

TOR5 (56–58). This "Ragulator" complex recruits Ragulator GTPases and V-ATPase to lysosomes, which further activate mTORC1 on the lysosomal surface in response to amino acids (58–60). Because NF1 specifically interacts with LAMTOR1 but not with any other mTOR signaling pathway key components, we determined whether NF1 regulates mTOR signaling through LAMTOR1. Using a well characterized mTOR substrate, S6 kinase (S6K) Thr-389 phosphorylation, we evaluated mTOR signaling activation in response to amino acids in HeLa and HeLa-NF1-KO cells. Indeed, we found that S6K phosphorylation was enhanced in HeLa-NF1-KO cells, indicating that NF1 inhibits mTOR signaling (Fig. 6*A*). Knocking down LAMTOR1 reduced the level of phospho-S6K in both HeLa and HEK293T cells, indicating that mTOR signaling hyperactivation in NF1-KO cells depends on LAMTOR1 (Fig. 6*B*).

To determine whether the cell growth and survival of NF1-deficient cells have become dependent on hyperactivation of the mTOR pathway, we treated these eight cell lines with different doses of rapamycin (Fig. 6*C*). We found that, compared with their parental cell lines, the proliferation of both HeLa-NF1-KO and HEK293T-NF1-KO cells was suppressed

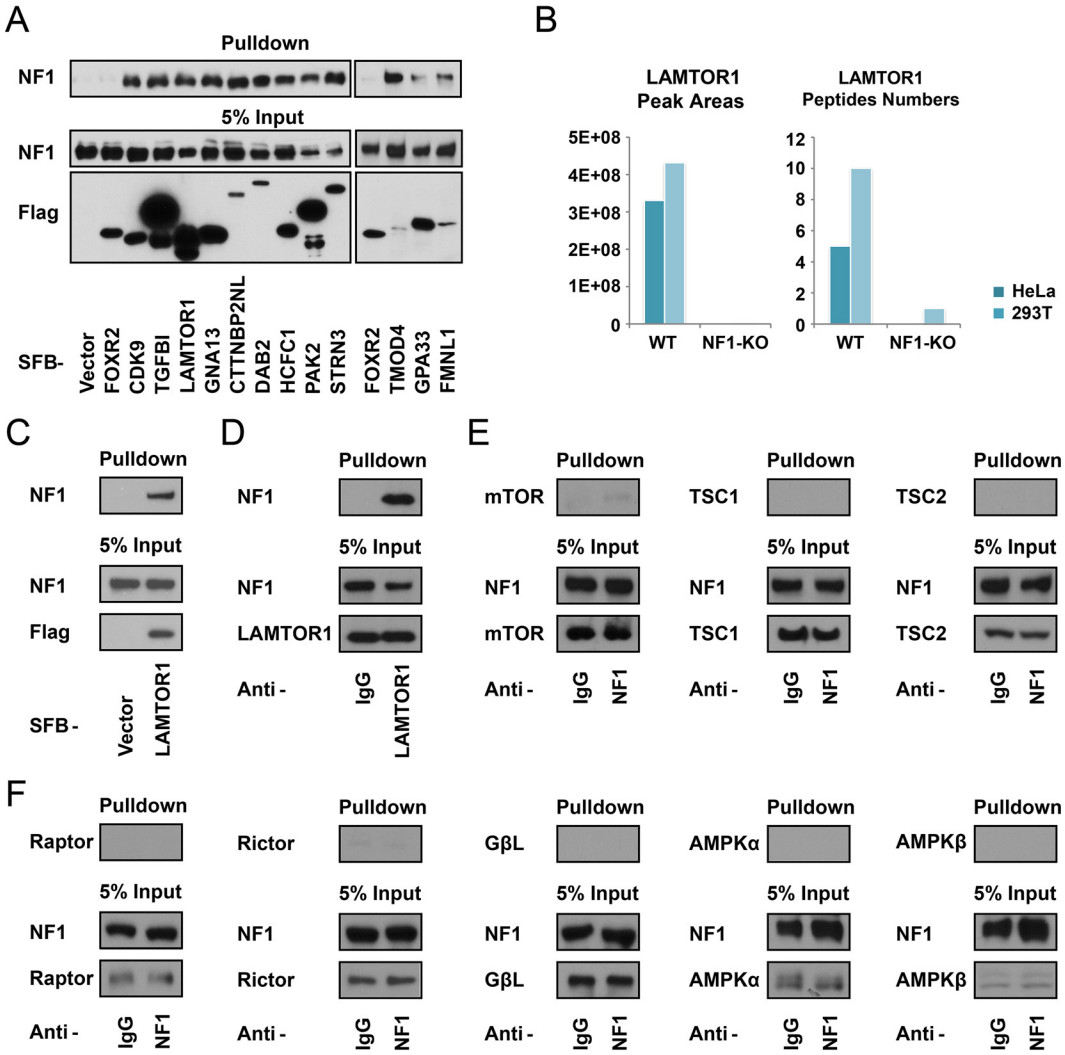

FIG. 5. **NF1 forms an endogenous protein complex with LAMTOR1 in the mTOR signaling pathway.** *A,* validation of NF1 HCIPs. HEK293T cells were transfected with 12 SFB-tagged constructs encoding the indicated NF1 HCIP proteins, using empty vector and SFB-FOXR2 as negative controls. Pulldown experiments were performed using S-protein beads and blotted with antibodies recognizing the FLAG epitope tag or endogenous NF1. Five percent of the corresponding cell lysate used in the IP was included as the input control. All the HCIPs were able to pull down endogenous NF1. *B,* LAMTOR1 in NF1 AP-MS in HeLa, HeLa-NF1-KO, HEK293T, and HEK293T-NF1-KO cells was evaluated in peak areas and peptide numbers. *C,* HEK293T cells were transfected with SFB-tagged LAMTOR1, with empty vector as the negative control. Pulldown experiments were performed using S-protein beads and blotted with antibodies recognizing the FLAG-epitope tag or endogenous NF1. Five percent of the corresponding cell lysate used in the IP was included as the input control. *D,* reciprocal co-IP of endogenous LAMTOR1 with NF1 was performed with IgG or anti-LAMTOR1 antibody, using whole cell lysate prepared from HeLa cells. Five percent of the corresponding cell lysate used in the IP was included as the input control. *E* and *F,* co-IP of other mTOR signaling pathway components with NF1 was performed with IgG or anti-mTOR, anti-TSC1, anti-TSC2, anti-Raptor, anti-Rictor, anti-GβL, anti-AMPKα1/2, or anti-AMPKβ1/2 antibodies, using whole cell lysate prepared from HeLa cells. Five percent of the corresponding cell lysate used in the IP was included as the input control.

after rapamycin treatment (HEK293T cells, 10 nM, $p < 0.01$; 100 nM and 1 μM, $p < 0.001$; HeLa cells: 100 nM and 1 μM, $p < 0.01$) (Fig. 6*C*). Knock down of LAMTOR1 rescued this effect in both cell lines (HEK293T cells: 10 and 100 nM and 1 μM, $p < 0.001$; HeLa cells: 100 nM, $p < 0.01$; 1 μM, $p < 0.05$), indicating that NF1-KO-induced mTOR signaling hyperactivation is LAMTOR1-dependent (Fig. 6*C*). A soft agar colony formation assay also confirmed that LAMTOR1 is very important for the tumorigenic properties of NF1-deficient cells. HeLa-NF1-KO cells form significantly more colonies than do HeLa cells ($p < 0.01$), whereas knockdown of LAMTOR1 almost abolished this effect ($p < 0.01$) (Fig. 6*D*). Collectively, these results indicate that NF1 forms a protein complex with LAMTOR1 and inhibits mTOR signaling in a LAMTOR1-dependent manner (Fig. 6*E*).

DISCUSSION

Considerable efforts have been devoted to MS data analysis for the identification of *bona fide* associated proteins (61,

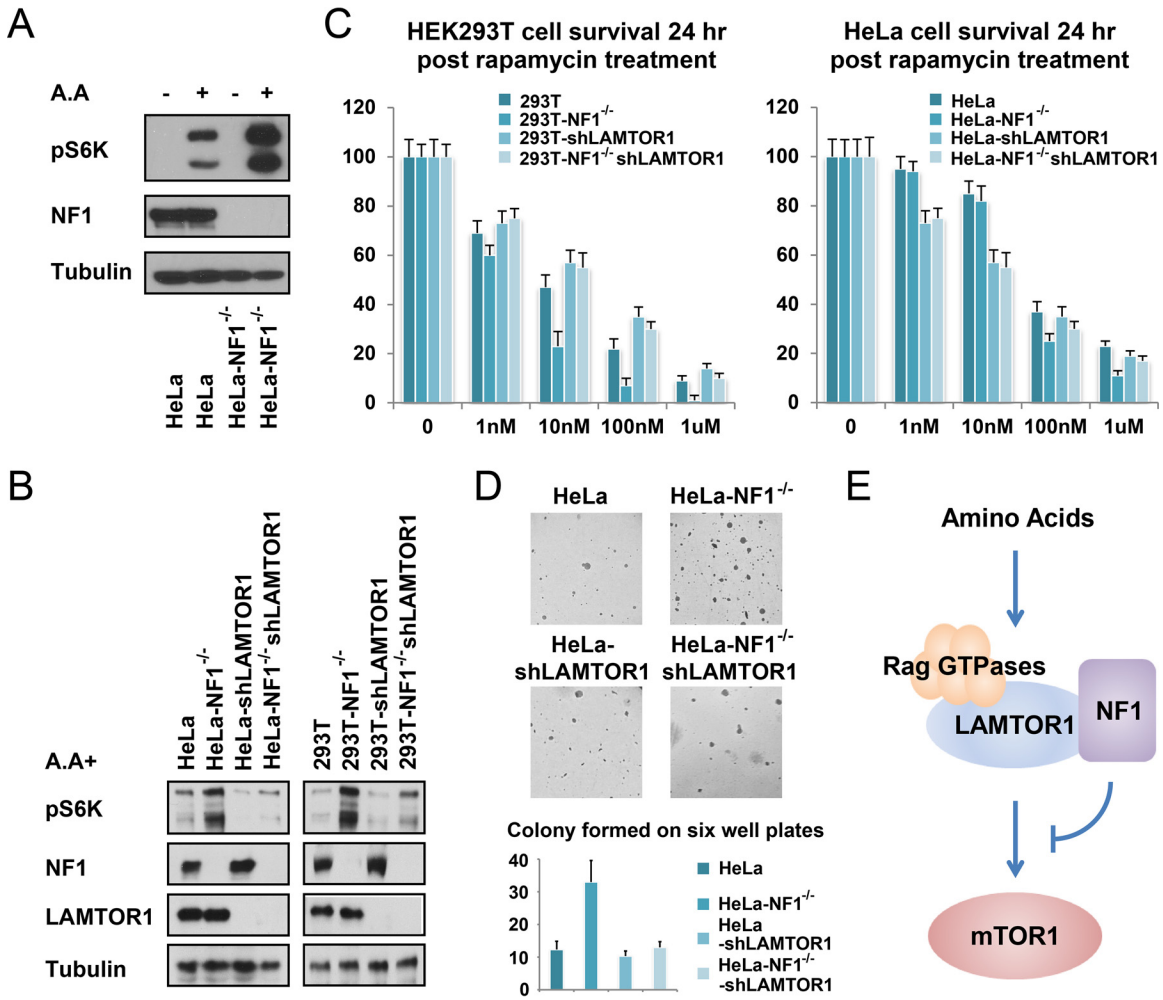

FIG. 6. **NF1 regulates mTOR signaling in a LAMTOR1-dependent manner.** *A,* HeLa and HeLa-NF1-KO cells were cultured in amino acid-free medium for 24 h and replaced with fresh amino acid-free medium or regular medium with 10% FBS. Cell lysates were collected and blotted with antibodies, as indicated. *B,* HeLa, HeLa-NF1-KO, HeLa-shLAMTOR1, HeLa-NF1-KO-shLAMTOR1, HEK293T, HEK293T-NF1-KO, HEK293T-shLAMTOR1, and HEK293T-NF1-KO-shLAMTOR1 cells were cultured in amino acid-free medium for 24 h and replaced with regular medium with 10% FBS. Cell lysates were collected, and a Western blotting analysis was performed using the antibodies, as indicated. *C,* eight cell lines were serum-starved and treated with rapamycin at the indicated concentration for 24 h, followed by a 3-(4,5-dimethylthiazol-2-yl)-2,5-diphenyltetrazolium bromide assay to assess cell viability. *D,* soft agar colony formation assay of HeLa, HeLa-NF1-KO, HeLa-shLAMTOR1, and HeLa-NF1-KO-shLAMTOR1 cells. *E,* working model showing that NF1 binds to LAMTOR1 and inhibits mTOR1 signaling.

62). It is challenging to choose the right interactions from the many false positives for in-depth functional analysis. Many algorithms have been proposed to identify *bona fide* interactions while eliminating false-positive results (43, 48, 63–67). Choosing and efficiently using these algorithms requires extensive experience in AP-MS and a large amount of work to accumulate the reference datasets in any given cells (68). The ACUMEN method that we developed here requires a simple comparison between WT and KO cells and an evaluation of the ratio and *p* value, with no mathematical model; we hope this technique will relieve researchers from having to perform complicated data analyses.

Some proteins, such as 14-3-3 family members (69) and many deubiquitinases (70), are known to regulate diverse cellular functions. However, due to their high abundance and frequent appearance in AP-MS results, they are recognized as contaminants when using most frequency analysis-based data analysis tools. The ACUMEN method could partially solve this problem. For example, NF1 is known to be regulated by 14-3-3 proteins (71). In our study, 14-3-3 proteins were identified in IP complexes from both WT and KO cells. However, they were significantly ($p < 0.01$) enriched in IP complexes from HEK293T cells (YWHAB, 3.6-fold; YWHAH, 2-fold) compared with those from HEK293T-NF1-KO cells. Although such enrichments were barely statistically significant in HeLa label-free results (YWHAB, 1.6-fold, $p < 0.05$; YWHAH, 1.7-fold, $p < 0.2$), the use of SILAC-ACUMEN in HeLa cells confirmed these data. These results indicate that a case-by-case analysis of AP-MS results will make it easier to choose the correct proteins of interest for in-depth functional

studies. Note that it is important to have a very clear biological question in mind when conducting these studies.

There are several approaches available for introducing the Cas9 system into target cells (72–74). For the ACUMEN system, the ideal method is to use transient transfection to introduce plasmids containing Cas9 and sgRNAs, as we did in this study, because continued expression of the CRISPR components is no longer necessary once gene editing has been completed (75). However, using a lentiviral or retroviral system for CRISPR/Cas9 delivery is beneficial in other cell lines that are difficult to transfect. Developing a stable Cas9 effector cell line using lentiviral or retroviral vectors before introducing sgRNAs can be an easier way when studying several proteins in the same cell system, because it simplifies the procedure for a larger scale study. It is challenging to generate CRISPR/Cas9 knock-out cells in primary cells. An alternative approach is to use purified Cas9-sgRNA ribonucleoproteins for delivery. Electroporation methods have been established to introduce Cas9-sgRNA complexes into primary cells and embryonic stem cells, and these can induce targeted gene mutations and large chromosome deletions while minimizing off-target effects (76–79). With the development of CRISPR/Cas9 gene editing technology, we hope that the ACUMEN system will be adopted for studies in all cell lines or even animal models in the future.

The ACUMEN method is limited by the availability of specific antibodies that recognize a particular target protein. Although cross-reaction is no longer the major issue for ACUMEN when choosing antibodies, the potency of antibodies to enrich for the bait protein is still a major consideration. Of note, although the ACUMEN method provides a good assessment of the nonspecific associations with the individual antibody used, it may not draw a complete picture of the isolated protein complex of interest because certain antibodies may bind to a particular protein surface and therefore prevent it from forming complexes with other proteins. Thus, using more than one antibody that recognizes different epitopes or surfaces of the bait protein will help to achieve full coverage of its interacting proteins. The newly developed CRISPR/Cas9 knock-in system also provides an alternative solution (80). Using the Cas9-induced DNA double strand breaks that can be repaired by homologous recombination, epitope tags can be knocked into the locus of the bait protein, which would allow researchers to use the existing anti-epitope antibodies (*e.g.* GFP, FLAG, and HA) to perform these endogenous AP-MS studies (81). Although this approach would still pull down nonspecific abundant proteins and tag-specific contaminants, similar to other AP-MS methods using epitope tags, it provides a more convenient method of performing genome-wide endogenous protein complex screening, which does not rely on the availability of antibodies against endogenous proteins.

Unlike other AP-MS methods that have been used extensively in large scale studies of mammalian cells and have resulted in many publicly available datasets, such as FLAG tag-based AP-MS, ACUMEN is a new method, with no comparable results generated using similar approaches in previous AP-MS-based PPI networks. This makes it difficult to evaluate the data quality of individual ACUMEN results by comparing them with knowledge-based AP-MS database results. Including pre-existing PPI information into endogenous protein networks established by ACUMEN would be helpful but could also be risky, because many previous studies used IgG pulldown or empty vector-transfected cells as controls. After many years of AP-MS data analysis, researchers have realized that these are "imperfect controls" that generate many false-positive results, because the total number of identifications in these control experiments is much lower than is that in real experiments (82, 83).

In this study, we found that more than half of the previously reported NF1-specific interacting proteins that were identified using the original filtration methods may be false positives (Fig. 3*H* and supplemental Table 6). Further analysis of these results revealed that these false-positive identifications were mostly generated from studies using imperfect controls, as described above, whereas most previous TAP-MS results were reproducible because they used stringent two-step AP protocols. However, these differences could also be due to the different cell systems or lysis buffers used in different studies. Eighteen percent of the previously reported NF1-interacting proteins were not detectable in at least one of the two cell lines we used, and 28% of the previously reported proteins passed our specificity filtration criteria in only one cell line (supplemental Table 6). These results indicate that cell line differences, especially protein abundance differences, may affect the levels of nonspecific associations as well as the formation of cell-specific protein interactions. Similarly, different sample preparing protocols, such as using different lysis buffers, could also greatly impact the levels of nonspecific associations (84). Thus, we need to be very cautious about what information is incorporated into the new endogenous PPI networks generated using the ACUMEN method.

Collectively, the CRISPR/Cas9-coupled AP-MS ACUMEN method provides a rapid and technically convenient approach to uncovering endogenous protein complexes of any given protein in any given cell type. Compared with previous approaches, this method can identify weak but *bona fide* interactions, such as NF1-KRAS association, from significant background noise. Using quantitative MS is helpful but is no longer required. Obtaining high quality antibodies with little cross-reaction is no longer required, because the cross-reaction can be easily eliminated using the ACUMEN method. The post-MS data analysis has been significantly simplified and no longer requires data accumulation in the cell of interest. With the establishment of genome-wide CRISPR gRNA libraries (85), this approach could be adopted to larger scale PPI studies, such as proteomics studies of protein families or signaling pathways involved in important biological processes (37, 49).

Using the ACUMEN system, we found a novel NF1-interacting protein, LAMTOR1, and linked its interaction with mTOR signaling activation (Figs. 5 and 6). LAMTOR1 has been known as the anchor protein of the Ragulator complex on the lysosome surface, which recruits Ragulator GTPases and other GTPases to lysosomes, presumably in response to amino acids (56–60). Because NF1 is a GTPase-activating protein that accelerates RAS GTPase hydrolysis and inhibits its activation (2, 9), it may also regulate Rag GTPases or other GTPases recruited by LAMTOR1 through a similar mechanism. Identifying the exact substrates of NF1 in mTOR signaling may require extensive work and well designed biochemistry analyses; however, it may eventually establish mechanistic associations between the two important cancer-related signaling pathways and suggest novel treatments for NF1 or mTOR-related tumors.

GTPases are a large family of hydrolase enzymes that can regulate signal cascades through their abilities of binding and hydrolyzing GTP. They can be inactivated by GTPase-activating proteins such as NF1, switching the GTPases from GTP-bound form to GDP-bound form. They can also be reactivated by guanine nucleotide exchange factors, which dissociate the GDP from the GTPase. In our studies, in addition to LAMTOR1, we have also identified many other novel NF1-interacting proteins, including the GTPase-regulating guanine nucleotide exchange factors RAPGEF2, RAPGEF6, and Trio; the Rho GTPase-activating protein ARHGAP17; and other GTPase-interacting proteins, such as GNA13, MPRIP, ERC1, and PAK2 (supplemental Table 2). These proteins are likely to form GTPase-regulating complexes, which may coordinately modulate GTPase activities both positively and negatively. Further investigation of these interactions and in-depth functional studies may provide more novel insights into the regulations of GTPases in different signaling cascades.

DATA AVAILABILITY

The mass spectrometry proteomics data have been deposited to the ProteomeXchange Consortium (http://proteomecentral.proteomexchange.org) via the PRIDE partner repository (Hinxton, UK) (86) with the dataset identifier PXD005107. Project Name, AP-MS in CRISPR/Cas9 Utilizing Systems for Mapping Endogenous Protein Complexes Interaction Network. Project accession no., PXD005107; Project DOI, 10.6019/PXD005107.

Acknowledgments—We thank the Chen, Wang, and Qin laboratories for their advice and technical assistance and Markeda Wade and Ann Sutton for editing the manuscript. The University of Texas MD Anderson Cancer Center is supported by National Institutes of Health Core Grant CA016672.

* This work was supported in part with a startup fund from the University of Texas MD Anderson Cancer Center and Era of Hope Scholar Research Award W81XWH-09-1-0409 from the United States Department of Defense (to J. Chen). The authors declare that they have no conflicts of interest with the contents of this article. The content is solely the responsibility of the authors and does not necessarily represent the official views of the National Institutes of Health.

S This article contains supplemental material.

§ Both authors contributed equally to this work.

¶ Recipient of a Computational Cancer Biology Training Program Fellowship supported by the Cancer Prevention and Research Institute of Texas.

§§ Recipient of an American Association For Cancer Research Career Development Award for Translational Breast Cancer Research, supported by the Breast Cancer Research Foundation.

¶¶ To whom correspondence should be addressed. E-mail: jchen8@mdanderson.org; E-mail: yiw@bcm.edu, and E-mail: wenqiw6@uci.edu.

REFERENCES

1. Rasmussen, S. A., and Friedman, J. M. (2000) NF1 gene and neurofibromatosis 1. *Am. J. Epidemiol.* **151,** 33–40
2. Xu, G. F., O'Connell, P., Viskochil, D., Cawthon, R., Robertson, M., Culver, M., Dunn, D., Stevens, J., Gesteland, R., and White, R. (1990) The neurofibromatosis type 1 gene encodes a protein related to GAP. *Cell* **62,** 599–608
3. Farid, M., Demicco, E. G., Garcia, R., Ahn, L., Merola, P. R., Cioffi, A., and Maki, R. G. (2014) Malignant peripheral nerve sheath tumors. *Oncologist* **19,** 193–201
4. Cancer Genome Atlas Research Network. (2008) Comprehensive genomic characterization defines human glioblastoma genes and core pathways. *Nature* **455,** 1061–1068
5. Krauthammer, M., Kong, Y., Bacchiocchi, A., Evans, P., Pornputtapong, N., Wu, C., McCusker, J. P., Ma, S., Cheng, E., Straub, R., Serin, M., Bosenberg, M., Ariyan, S., Narayan, D., Sznol, M., *et al.* (2015) Exome sequencing identifies recurrent mutations in NF1 and RASopathy genes in sun-exposed melanomas. *Nat. Genet.* **47,** 996–1002
6. Cancer Genome Atlas Research Network. (2011) Integrated genomic analyses of ovarian carcinoma. *Nature* **474,** 609–615
7. Ding, L., Getz, G., Wheeler, D. A., Mardis, E. R., McLellan, M. D., Cibulskis, K., Sougnez, C., Greulich, H., Muzny, D. M., Morgan, M. B., Fulton, L., Fulton, R. S., Zhang, Q., Wendl, M. C., Lawrence, M. S., *et al.* (2008) Somatic mutations affect key pathways in lung adenocarcinoma. *Nature* **455,** 1069–1075
8. Cancer Genome Atlas Network. (2012) Comprehensive molecular portraits of human breast tumours. *Nature* **490,** 61–70
9. Martin, G. A., Viskochil, D., Bollag, G., McCabe, P. C., Crosier, W. J., Haubruck, H., Conroy, L., Clark, R., O'Connell, P., and Cawthon, R. M. (1990) The GAP-related domain of the neurofibromatosis type 1 gene product interacts with ras p21. *Cell* **63,** 843–849
10. Basu, T. N., Gutmann, D. H., Fletcher, J. A., Glover, T. W., Collins, F. S., and Downward, J. (1992) Aberrant regulation of ras proteins in malignant tumour cells from type 1 neurofibromatosis patients. *Nature* **356,** 713–715
11. Yap, Y. S., McPherson, J. R., Ong, C. K., Rozen, S. G., Teh, B. T., Lee, A. S., and Callen, D. F. (2014) The NF1 gene revisited-from bench to bedside. *Oncotarget* **5,** 5873–5892
12. Ratner, N., and Miller, S. J. (2015) A RASopathy gene commonly mutated in cancer: the neurofibromatosis type 1 tumour suppressor. *Nat. Rev. Cancer* **15,** 290–301
13. Aebersold, R., and Mann, M. (2003) Mass spectrometry-based proteomics. *Nature* **422,** 198–207
14. Altelaar, A. F., Munoz, J., and Heck, A. J. (2013) Next-generation proteomics: toward an integrative view of proteome dynamics. *Nat. Rev. Genet.* **14,** 35–48
15. Knuesel, M., Wan, Y., Xiao, Z., Holinger, E., Lowe, N., Wang, W., and Liu, X. (2003) Identification of novel protein-protein interactions using a versatile mammalian tandem affinity purification expression system. *Mol. Cell. Proteomics* **2,** 1225–1233
16. Luo, Q., Nieves, E., Kzhyshkowska, J., and Angeletti, R. H. (2006) Endogenous transforming growth factor-β receptor-mediated Smad signaling complexes analyzed by mass spectrometry. *Mol. Cell. Proteomics* **5,** 1245–1260
17. Brown, K. A., Ham, A. J., Clark, C. N., Meller, N., Law, B. K., Chytil, A., Cheng, N., Pietenpol, J. A., and Moses, H. L. (2008) Identification of novel

Smad2 and Smad3 associated proteins in response to TGF-β1. *J. Cell. Biochem.* **105,** 596–611
18. Chaudhry, S. S., Cain, S. A., Morgan, A., Dallas, S. L., Shuttleworth, C. A., and Kielty, C. M. (2007) Fibrillin-1 regulates the bioavailability of TGFβ1. *J. Cell Biol.* **176,** 355–367
19. Conrotto, P., Yakymovych, I., Yakymovych, M., and Souchelnytskyi, S. (2007) Interactome of transforming growth factor-β type I receptor (TβRI): inhibition of TGFβ signaling by Epac1. *J. Proteome Res.* **6,** 287–297
20. Angers, S., Thorpe, C. J., Biechele, T. L., Goldenberg, S. J., Zheng, N., MacCoss, M. J., and Moon, R. T. (2006) The KLHL12-Cullin-3 ubiquitin ligase negatively regulates the Wnt-β-catenin pathway by targeting Dishevelled for degradation. *Nat. Cell Biol.* **8,** 348–357
21. Major, M. B., Camp, N. D., Berndt, J. D., Yi, X., Goldenberg, S. J., Hubbert, C., Biechele, T. L., Gingras, A. C., Zheng, N., Maccoss, M. J., Angers, S., and Moon, R. T. (2007) Wilms tumor suppressor WTX negatively regulates WNT/β-catenin signaling. *Science* **316,** 1043–1046
22. Huen, M. S., Grant, R., Manke, I., Minn, K., Yu, X., Yaffe, M. B., and Chen, J. (2007) RNF8 transduces the DNA-damage signal via histone ubiquitylation and checkpoint protein assembly. *Cell* **131,** 901–914
23. Liu, T., Ghosal, G., Yuan, J., Chen, J., and Huang, J. (2010) FAN1 acts with FANCI-FANCD2 to promote DNA interstrand cross-link repair. *Science* **329,** 693–696
24. Yu, X., Chini, C. C., He, M., Mer, G., and Chen, J. (2003) The BRCT domain is a phospho-protein binding domain. *Science* **302,** 639–642
25. Lou, Z., Minter-Dykhouse, K., Wu, X., and Chen, J. (2003) MDC1 is coupled to activated CHK2 in mammalian DNA damage response pathways. *Nature* **421,** 957–961
26. Kim, J. E., Chen, J., and Lou, Z. (2008) DBC1 is a negative regulator of SIRT1. *Nature* **451,** 583–586
27. Gibson, T. J., Seiler, M., and Veitia, R. A. (2013) The transience of transient overexpression. *Nat Methods* **10,** 715–721
28. Braun, P., Cusick, M. E., and Vidal, M. (2006) QUICKstep and GS-TAP: new moves for protein-interaction analysis. *Nat. Methods* **3,** 975–976
29. Blagoev, B., Kratchmarova, I., Ong, S. E., Nielsen, M., Foster, L. J., and Mann, M. (2003) A proteomics strategy to elucidate functional protein-protein interactions applied to EGF signaling. *Nat. Biotechnol.* **21,** 315–318
30. Tackett, A. J., DeGrasse, J. A., Sekedat, M. D., Oeffinger, M., Rout, M. P., and Chait, B. T. (2005) I-DIRT, a general method for distinguishing between specific and nonspecific protein interactions. *J. Proteome Res.* **4,** 1752–1756
31. Ranish, J. A., Yi, E. C., Leslie, D. M., Purvine, S. O., Goodlett, D. R., Eng, J., and Aebersold, R. (2003) The study of macromolecular complexes by quantitative proteomics. *Nat. Genet.* **33,** 349–355
32. Selbach, M., and Mann, M. (2006) Protein interaction screening by quantitative immunoprecipitation combined with knockdown (QUICK). *Nat. Methods* **3,** 981–983
33. Trinkle-Mulcahy, L., Boulon, S., Lam, Y. W., Urcia, R., Boisvert, F. M., Vandermoere, F., Morrice, N. A., Swift, S., Rothbauer, U., Leonhardt, H., and Lamond, A. (2008) Identifying specific protein interaction partners using quantitative mass spectrometry and bead proteomes. *J. Cell Biol.* **183,** 223–239
34. Jinek, M., Chylinski, K., Fonfara, I., Hauer, M., Doudna, J. A., and Charpentier, E. (2012) A programmable dual-RNA-guided DNA endonuclease in adaptive bacterial immunity. *Science* **337,** 816–821
35. Cong, L., Ran, F. A., Cox, D., Lin, S., Barretto, R., Habib, N., Hsu, P. D., Wu, X., Jiang, W., Marraffini, L. A., and Zhang, F. (2013) Multiplex genome engineering using CRISPR/Cas systems. *Science* **339,** 819–823
36. Mali, P., Yang, L., Esvelt, K. M., Aach, J., Guell, M., DiCarlo, J. E., Norville, J. E., and Church, G. M. (2013) RNA-guided human genome engineering via Cas9. *Science* **339,** 823–826
37. Li, X., Wang, W., Wang, J., Malovannaya, A., Xi, Y., Li, W., Guerra, R., Hawke, D. H., Qin, J., and Chen, J. (2015) Proteomic analyses reveal distinct chromatin-associated and soluble transcription factor complexes. *Mol. Syst. Biol.* **11,** 775
38. Nesvizhskii, A. I., and Aebersold, R. (2005) Interpretation of shotgun proteomic data: the protein inference problem. *Mol. Cell. Proteomics* **4,** 1419–1440
39. MacLean, B., Tomazela, D. M., Shulman, N., Chambers, M., Finney, G. L., Frewen, B., Kern, R., Tabb, D. L., Liebler, D. C., and MacCoss, M. J. (2010) Skyline: an open source document editor for creating and analyzing targeted proteomics experiments. *Bioinformatics* **26,** 966–968
40. Abbatiello, S. E., Schilling, B., Mani, D. R., Zimmerman, L. J., Hall, S. C., MacLean, B., Albertolle, M., Allen, S., Burgess, M., Cusack, M. P., Gosh, M., Hedrick, V., Held, J. M., Inerowicz, H. D., Jackson, A., *et al.* (2015) Large-scale interlaboratory study to develop, analytically validate and apply highly multiplexed, quantitative peptide assays to measure cancer-relevant proteins in plasma. *Mol. Cell. Proteomics* **14,** 2357–2374
41. UniProt Consortium. (2012) Reorganizing the protein space at the Universal Protein Resource (UniProt). *Nucleic Acids Res.* **40,** D71–D75
42. Smoot, M. E., Ono, K., Ruscheinski, J., Wang, P. L., and Ideker, T. (2011) Cytoscape 2.8: new features for data integration and network visualization. *Bioinformatics* **27,** 431–432
43. Malovannaya, A., Lanz, R. B., Jung, S. Y., Bulynko, Y., Le, N. T., Chan, D. W., Ding, C., Shi, Y., Yucer, N., Krenciute, G., Kim, B. J., Li, C., Chen, R., Li, W., Wang, Y., O'Malley, B. W., and Qin, J. (2011) Analysis of the human endogenous coregulator complexome. *Cell* **145,** 787–799
44. Malovannaya, A., Li, Y., Bulynko, Y., Jung, S. Y., Wang, Y., Lanz, R. B., O'Malley, B. W., and Qin, J. (2010) Streamlined analysis schema for high-throughput identification of endogenous protein complexes. *Proc. Natl. Acad. Sci. U.S.A.* **107,** 2431–2436
45. Perkins, D. N., Pappin, D. J., Creasy, D. M., and Cottrell, J. S. (1999) Probability-based protein identification by searching sequence databases using mass spectrometry data. *Electrophoresis* **20,** 3551–3567
46. Rigaut, G., Shevchenko, A., Rutz, B., Wilm, M., Mann, M., and Séraphin, B. (1999) A generic protein purification method for protein complex characterization and proteome exploration. *Nat. Biotechnol.* **17,** 1030–1032
47. Couzens, A. L., Knight, J. D., Kean, M. J., Teo, G., Weiss, A., Dunham, W. H., Lin, Z. Y., Bagshaw, R. D., Sicheri, F., Pawson, T., Wrana, J. L., Choi, H., and Gingras, A. C. (2013) Protein interaction network of the mammalian Hippo pathway reveals mechanisms of kinase-phosphatase interactions. *Sci. Signal.* **6,** rs15
48. Sowa, M. E., Bennett, E. J., Gygi, S. P., and Harper, J. W. (2009) Defining the human deubiquitinating enzyme interaction landscape. *Cell* **138,** 389–403
49. Wang, W., Li, X., Huang, J., Feng, L., Dolinta, K. G., and Chen, J. (2014) Defining the protein-protein interaction network of the human hippo pathway. *Mol. Cell. Proteomics* **13,** 119–131
50. Gandhi, T. K., Zhong, J., Mathivanan, S., Karthick, L., Chandrika, K. N., Mohan, S. S., Sharma, S., Pinkert, S., Nagaraju, S., Periaswamy, B., Mishra, G., Nandakumar, K., Shen, B., Deshpande, N., Nayak, R., *et al.* (2006) Analysis of the human protein interactome and comparison with yeast, worm and fly interaction datasets. *Nat. Genet.* **38,** 285–293
51. Lawrence, M. S., Stojanov, P., Mermel, C. H., Robinson, J. T., Garraway, L. A., Golub, T. R., Meyerson, M., Gabriel, S. B., Lander, E. S., and Getz, G. (2014) Discovery and saturation analysis of cancer genes across 21 tumour types. *Nature* **505,** 495–501
52. Ross, P. L., Huang, Y. N., Marchese, J. N., Williamson, B., Parker, K., Hattan, S., Khainovski, N., Pillai, S., Dey, S., Daniels, S., Purkayastha, S., Juhasz, P., Martin, S., Bartlet-Jones, M., He, F., Jacobson, A., and Pappin, D. J. (2004) Multiplexed protein quantitation in *Saccharomyces cerevisiae* using amine-reactive isobaric tagging reagents. *Mol. Cell. Proteomics* **3,** 1154–1169
53. Dayon, L., Hainard, A., Licker, V., Turck, N., Kuhn, K., Hochstrasser, D. F., Burkhard, P. R., and Sanchez, J. C. (2008) Relative quantification of proteins in human cerebrospinal fluids by MS/MS using 6-plex isobaric tags. *Anal. Chem.* **80,** 2921–2931
54. Thompson, A., Schäfer, J., Kuhn, K., Kienle, S., Schwarz, J., Schmidt, G., Neumann, T., Johnstone, R., Mohammed, A. K., and Hamon, C. (2003) Tandem mass tags: a novel quantification strategy for comparative analysis of complex protein mixtures by MS/MS. *Anal. Chem.* **75,** 1895–1904
55. Johannessen, C. M., Reczek, E. E., James, M. F., Brems, H., Legius, E., and Cichowski, K. (2005) The NF1 tumor suppressor critically regulates TSC2 and mTOR. *Proc. Natl. Acad. Sci. U.S.A.* **102,** 8573–8578
56. Hoshino, D., Tomari, T., Nagano, M., Koshikawa, N., and Seiki, M. (2009) A novel protein associated with membrane-type 1 matrix metalloproteinase binds p27(kip1) and regulates RhoA activation, actin remodeling, and Matrigel invasion. *J. Biol. Chem.* **284,** 27315–27326
57. Soma-Nagae, T., Nada, S., Kitagawa, M., Takahashi, Y., Mori, S., Oneyama, C., and Okada, M. (2013) The lysosomal signaling anchor

p18/LAMTOR1 controls epidermal development by regulating lysosome-mediated catabolic processes. *J. Cell Sci.* **126,** 3575–3584
58. Nada, S., Mori, S., Takahashi, Y., and Okada, M. (2014) p18/LAMTOR1: a late endosome/lysosome-specific anchor protein for the mTORC1/MAPK signaling pathway. *Methods Enzymol.* **535,** 249–263
59. Sancak, Y., Bar-Peled, L., Zoncu, R., Markhard, A. L., Nada, S., and Sabatini, D. M. (2010) Ragulator-Rag complex targets mTORC1 to the lysosomal surface and is necessary for its activation by amino acids. *Cell* **141,** 290–303
60. Bar-Peled, L., Schweitzer, L. D., Zoncu, R., and Sabatini, D. M. (2012) Ragulator is a GEF for the rag GTPases that signal amino acid levels to mTORC1. *Cell* **150,** 1196–1208
61. Nesvizhskii, A. I., Vitek, O., and Aebersold, R. (2007) Analysis and validation of proteomic data generated by tandem mass spectrometry. *Nat Methods* **4,** 787–797
62. Matthiesen, R., Azevedo, L., Amorim, A., and Carvalho, A. S. (2011) Discussion on common data analysis strategies used in MS-based proteomics. *Proteomics* **11,** 604–619
63. Sardiu, M. E., Cai, Y., Jin, J., Swanson, S. K., Conaway, R. C., Conaway, J. W., Florens, L., and Washburn, M. P. (2008) Probabilistic assembly of human protein interaction networks from label-free quantitative proteomics. *Proc. Natl. Acad. Sci. U.S.A.* **105,** 1454–1459
64. Choi, H., Larsen, B., Lin, Z. Y., Breitkreutz, A., Mellacheruvu, D., Fermin, D., Qin, Z. S., Tyers, M., Gingras, A. C., and Nesvizhskii, A. I. (2011) SAINT: probabilistic scoring of affinity purification-mass spectrometry data. *Nat. Methods* **8,** 70–73
65. Guruharsha, K. G., Rual, J. F., Zhai, B., Mintseris, J., Vaidya, P., Vaidya, N., Beekman, C., Wong, C., Rhee, D. Y., Cenaj, O., McKillip, E., Shah, S., Stapleton, M., Wan, K. H., Yu, C., *et al.* (2011) A protein complex network of *Drosophila melanogaster*. *Cell* **147,** 690–703
66. Varjosalo, M., Sacco, R., Stukalov, A., van Drogen, A., Planyavsky, M., Hauri, S., Aebersold, R., Bennett, K. L., Colinge, J., Gstaiger, M., and Superti-Furga, G. (2013) Interlaboratory reproducibility of large-scale human protein-complex analysis by standardized AP-MS. *Nat. Methods* **10,** 307–314
67. Hauri, S., Wepf, A., van Drogen, A., Varjosalo, M., Tapon, N., Aebersold, R., and Gstaiger, M. (2013) Interaction proteome of human Hippo signaling: modular control of the co-activator YAP1. *Mol. Syst. Biol.* **9,** 713
68. Mellacheruvu, D., Wright, Z., Couzens, A. L., Lambert, J. P., St-Denis, N. A., Li, T., Miteva, Y. V., Hauri, S., Sardiu, M. E., Low, T. Y., Halim, V. A., Bagshaw, R. D., Hubner, N. C., Al-Hakim, A., Bouchard, A., *et al.* (2013) The CRAPome: a contaminant repository for affinity purification-mass spectrometry data. *Nat. Methods* **10,** 730–736
69. Mhawech, P. (2005) 14-3-3 proteins–an update. *Cell Res.* **15,** 228–236
70. Komander, D., Clague, M. J., and Urbé, S. (2009) Breaking the chains: structure and function of the deubiquitinases. *Nat. Rev. Mol. Cell Biol.* **10,** 550–563
71. Feng, L., Yunoue, S., Tokuo, H., Ozawa, T., Zhang, D., Patrakitkomjorn, S., Ichimura, T., Saya, H., and Araki, N. (2004) PKA phosphorylation and 14-3-3 interaction regulate the function of neurofibromatosis type I tumor suppressor, neurofibromin. *FEBS Lett.* **557,** 275–282
72. Wang, T., Wei, J. J., Sabatini, D. M., and Lander, E. S. (2014) Genetic screens in human cells using the CRISPR-Cas9 system. *Science* **343,** 80–84
73. Shalem, O., Sanjana, N. E., Hartenian, E., Shi, X., Scott, D. A., Mikkelsen, T. S., Heckl, D., Ebert, B. L., Root, D. E., Doench, J. G., and Zhang, F. (2014) Genome-scale CRISPR-Cas9 knock-out screening in human cells. *Science* **343,** 84–87
74. Sanjana, N. E., Shalem, O., and Zhang, F. (2014) Improved vectors and genome-wide libraries for CRISPR screening. *Nat. Methods* **11,** 783–784
75. Wang, H., La Russa, M., and Qi, L. S. (2016) CRISPR/Cas9 in genome editing and beyond. *Annu. Rev. Biochem.* **85,** 227–264
76. Kim, S., Kim, D., Cho, S. W., Kim, J., and Kim, J. S. (2014) Highly efficient RNA-guided genome editing in human cells via delivery of purified Cas9 ribonucleoproteins. *Genome Res.* **24,** 1012–1019
77. Liu, J., Gaj, T., Yang, Y., Wang, N., Shui, S., Kim, S., Kanchiswamy, C. N., Kim, J. S., and Barbas, C. F., 3rd. (2015) Efficient delivery of nuclease proteins for genome editing in human stem cells and primary cells. *Nat. Protoc.* **10,** 1842–1859
78. Schumann, K., Lin, S., Boyer, E., Simeonov, D. R., Subramaniam, M., Gate, R. E., Haliburton, G. E., Ye, C. J., Bluestone, J. A., Doudna, J. A., and Marson, A. (2015) Generation of knock-in primary human T cells using Cas9 ribonucleoproteins. *Proc. Natl. Acad. Sci. U.S.A.* **112,** 10437–10442
79. Hendel, A., Bak, R. O., Clark, J. T., Kennedy, A. B., Ryan, D. E., Roy, S., Steinfeld, I., Lunstad, B. D., Kaiser, R. J., Wilkens, A. B., Bacchetta, R., Tsalenko, A., Dellinger, D., Bruhn, L., and Porteus, M. H. (2015) Chemically modified guide RNAs enhance CRISPR-Cas genome editing in human primary cells. *Nat. Biotechnol.* **33,** 985–989
80. Dickinson, D. J., Ward, J. D., Reiner, D. J., and Goldstein, B. (2013) Engineering the *Caenorhabditis elegans* genome using Cas9-triggered homologous recombination. *Nat. Methods* **10,** 1028–1034
81. Dalvai, M., Loehr, J., Jacquet, K., Huard, C. C., Roques, C., Herst, P., Côté, J., and Doyon, Y. (2015) A scalable genome-editing-based approach for mapping multiprotein complexes in human cells. *Cell Rep.* **13,** 621–633
82. Gingras, A. C., Gstaiger, M., Raught, B., and Aebersold, R. (2007) Analysis of protein complexes using mass spectrometry. *Nat. Rev. Mol. Cell Biol.* **8,** 645–654
83. Keilhauer, E. C., Hein, M. Y., and Mann, M. (2015) Accurate protein complex retrieval by affinity enrichment mass spectrometry (AE-MS) rather than affinity purification mass spectrometry (AP-MS). *Mol. Cell. Proteomics* **14,** 120–135
84. Glatter, T., Ahrné, E., and Schmidt, A. (2015) Comparison of different sample preparation protocols reveals lysis buffer-specific extraction biases in Gram-negative bacteria and human cells. *J. Proteome Res.* **14,** 4472–4485
85. Koike-Yusa, H., Li, Y., Tan, E. P., Velasco-Herrera Mdel, C., and Yusa, K. (2014) Genome-wide recessive genetic screening in mammalian cells with a lentiviral CRISPR-guide RNA library. *Nat. Biotechnol.* **32,** 267–273
86. Vizcaíno, J. A., Côté, R. G., Csordas, A., Dianes, J. A., Fabregat, A., Foster, J. M., Griss, J., Alpi, E., Birim, M., Contell, J., O'Kelly, G., Schoenegger, A., Ovelleiro, D., Pérez-Riverol, Y., Reisinger, F., *et al.* (2013) The PRoteomics IDEntifications (PRIDE) database and associated tools: status in 2013. *Nucleic Acids Res.* **41,** D1063–D1069